Clays and Clay Minerals, Vol. 22, pp. 97–106. Pergamon Press 1974. Printed in Great Britain

FACTORS AFFECTING SELECTED AREA ELECTRON DIFFRACTION PATTERNS OF MICAS*

NECIP GÜVEN

Department of Geosciences, Texas Tech University,
P.O. Box 4109, Lubbock, Texas 79409, U.S.A.

(*Received* 27 *August* 1973)

Abstract—Major factors affecting the selected area electron diffraction (SAD) patterns of micas are: lattice properties of the crystal, specimen thickness, orientation of the crystal, properties of the Ewald sphere for electron diffraction, depth of field of the objective lens, and variations in focusing conditions of this lens. Depending on these factors, SAD patterns of $2M_1$ muscovite may display different symmetries. Specimen 'finite' thickness affects the intensity in terms of the 'interference function'. The latter function has been evaluated exactly and the intensity distribution has been calculated along the (*hk*) rows. The observed intensity variations of (*hk*) spots indicate that the focusing conditions of the objective lens are rather critical for the symmetry of SAD patterns.

INTRODUCTION

Selected area electron diffraction (SAD) gives information about the structure and morphology of a crystal from an area of about half a micron in diameter. The method therefore, has the promise of elucidating the crystal structure of fine-grained layer silicates like clay minerals. However, the potential of SAD has not been fully exploited in this regard, due mainly to the fact that the major factors affecting the SAD patterns have not been properly considered. These factors are: (1) lattice properties of the crystal; (2) properties of the Ewald sphere for electron diffraction; (3) crystal thickness; (4) orientation of the crystal with respect to the incident electron beam (tilt and bending); and (5) properties of the objective lens. These factors are generally well understood in terms of kinematical theory of electron diffraction and well-developed theories exist; e.g. Murr (1970), Cowley (1967), Pinsker (1953) and Vainstein (1964), among others. In this paper, the effects of the above factors will be specifically discussed with respect to $2M_1$ muscovite. The structure of this mica has been well determined by X-ray diffraction (Güven, 1971) and by neutron diffraction (Rothbauer, 1971).

LATTICE PROPERTIES OF MICAS

The reciprocal lattice plane (a^*c^*) of a hypothetical mica single layer is shown in Fig. 1a, where the **c***-direction is taken parallel to the electron beam. The magnitude of a reciprocal lattice vector $\mathbf{H}_{hkl}$ and that of its projection on the a–b plane can be calculated from the following relationships for a monoclinic crystal:

$$|\mathbf{H}_{hkl}|^2 = h^2a^{*2} + k^2b^{*2} + l^2c^{*2} + 2lhc^*a^*\cos\beta^*$$

$$|\text{proj.}\,\mathbf{H}_{hkl}|^2 = h^2a^{*2}\sin^2\beta^* + k^{*2}b^{*2}.$$

The distance Δp_{hkl} of a reciprocal lattice point above the a–b plane is given by the relationship:

$$\Delta p_{hkl} = |\mathbf{H}_{hkl}|^2 - |\text{proj.}\,\mathbf{H}_{hkl}|^2 = (ha^*\cos\beta^* + lc^*)^2;$$

replacing $\cos\beta^* = \dfrac{c^*}{3a^*}$, and expressing Δp_{hkl} in units of c^*:

$$\Delta p_{hkl} = \left(\frac{h}{3} + l\right)c^*.$$

This relationship states that all the reciprocal lattice points lying exactly on the a–b plane have h and l indices with $(h/3 + l) = 0$. Other reciprocal lattice points have a distance defined by Δp_{hkl} from that plane.

Stacking sequences in micas

Another complexity relates to the ability of micas and other layer silicates to form modifications with different stacking sequences. SAD patterns can reflect the appropriate symmetry if the 'finite' thickness of the crystal has an integral multiple of the number of layers in a stacking sequence. For instance, for a $3T$ mica a deviation from hexagonal symmetry may be expected if the number of layers is not $3n$. Similarly, for $2M_1$ muscovite the stacking sequence creates a glide plane which will show up as a mirror plane in the SAD pattern. If there is an odd number of layers, such as three or five, deviation from this mirror plane may be seen on the pattern.

* Dedicated to Late Professor W. F. Bradley who amply demonstrated the importance of mica structure to clay mineralogy.

https://doi.org/10.1346/CCMN.1974.0220114 Published online by Cambridge University Press

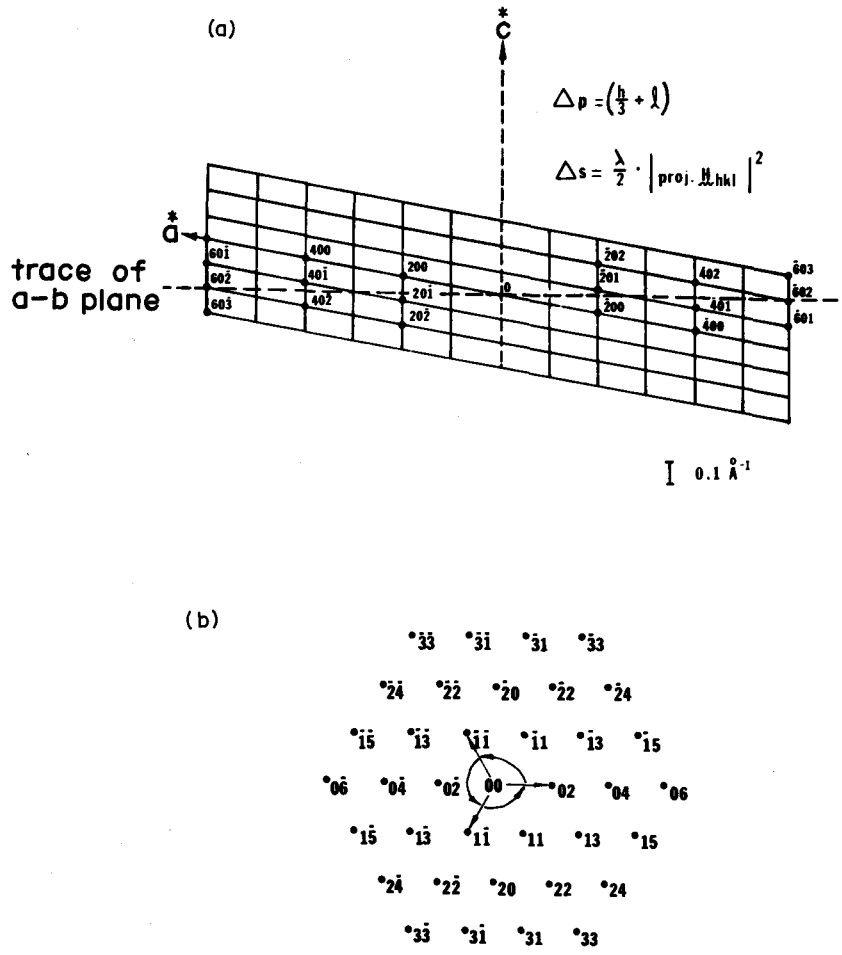


Fig. 1. Two projections of the reciprocal lattice of a mica single layer: (a) the a^*c^* reciprocal lattice plane and reciprocal lattice points close to the Ewald sphere, which almost coincides with the a–b plane; (b) the projection of the (hk) lattice rows onto the a–b plane of mica layer.

A completely random stacking sequence for a mica may give a hexagonal symmetry over the (hk) spots as the (hk) reciprocal lattice rows will superimpose on each other in the manner shown in Fig. 1(b). The calculation of the intensity variation along these rows is rather complicated. Since there are rather extensive treatments of this problem in the literature, it will not be discussed further in this paper.

PROPERTIES OF THE EWALD SPHERE FOR ELECTRON DIFFRACTION

It is well known that the Ewald sphere approximates rather closely a plane for electron diffraction. This plane is often considered to coincide with the a–b plane of the micas in the vicinity of the origin. The intensity of a reflection is a maximum at the exact Bragg condition and falls sharply with slight deviations from this position. It is, therefore, significant to know how much the Ewald sphere deviates from a plane. The amount of this deviation (Δs) is given by the following relationship:

$$\Delta s = |\text{proj. } \mathbf{H}_{hkl}| \tan \theta_{hkl},$$

but

$$\tan \theta_{hkl} \cong \frac{|\text{proj. } \mathbf{H}_{hkl}|}{2/\lambda},$$

$$\therefore \Delta s \cong \frac{\lambda}{2} |\text{proj. } \mathbf{H}_{hkl}|^2 \cong \frac{\lambda}{2}\left[\frac{h^2}{a^2} + \frac{k^2}{b^2}\right].$$

For an accelerating voltage of 80 keV, λ is 0·0418 Å and

$$\Delta s \cong 0{\cdot}02\, x |\text{proj. } \mathbf{H}_{hkl}|^2.$$

https://doi.org/10.1346/CCMN.1974.0220114 Published online by Cambridge University Press

As long as we limit our observations to that part of reciprocal space with $|\mathbf{H}_{hkl}| \leqslant 1{\cdot}0\,\text{Å}^{-1}$, the maximum deviation of the sphere from the a–b plane will be about $0{\cdot}02\,\text{Å}^{-1}$. For the (11) and (02) type reflections of a mica this deviation will be about $0{\cdot}001\,\text{Å}^{-1}$. It is more practical to give the deviation Δs in fractions of reciprocal lattice parameters in this direction: $\Delta s' = \Delta s/c^*$. Thus, the exact distance of a reciprocal lattice point from the sphere of reflection is $\zeta_{hkl} = \Delta p - \Delta s'$. Note that the ζ_{hkl} is given in fractions of reciprocal cell parameter. This distance is also referred to as the 'excitation error'.

In the above discussion, the spread of electron energies due to fluctuations in the accelerating voltage has been considered negligible, which is correct for modern electron microscopes. However, it may be worthwhile mentioning the effect of the beam divergence on the Ewald sphere. The beam incident on the specimen consists of a narrow cone defined by the radius of the condenser aperture and the focal length of the condenser lens. In modern instruments, the minimum angle of this convergence varies between $1\text{–}2 \times 10^{-3}$ rad. As a result, the sphere of reflection consists of a shell with a width (Δw) which increases with increasing diffraction angle. It can be shown that the ratio $\Delta s/\Delta w \simeq 10x|\text{proj. }\mathbf{H}_{hkl}|$ at 80 keV for a condenser aperture angle of 2×10^{-3} rad. For practical purposes, the beam divergence can therefore be neglected.

CRYSTAL THICKNESS

The effect of the crystal thickness on the electron diffraction pattern is fairly well understood in terms of the shape transform–elongation of the reciprocal lattice points. The thickness of a crystal in a given direction is defined by the number of unit-cells in that direction. The intensity of a reflection is then the product of two functions:

$$I \alpha F^2 \times S^2.$$

F is the well-known structure factor, which is the scattering amplitude from the n atoms in the unit-cell:

$$F = \sum_n f_n e^{2\pi i \mathbf{r}_n \cdot \mathbf{s}}.$$

S represents, on the other hand, the so-called "interference function" between all the unit-cells whose origins are related to a common origin by the vector:

$$\mathbf{R} = m_1\mathbf{a} + m_2\mathbf{b} + m_3\mathbf{c}.$$

The interference function is then given by the following expression:

$$S = \sum_{m_1} e^{2\pi i m_1 \mathbf{a}.\mathbf{s}} \sum_{m_2} e^{2\pi i m_2 \mathbf{b}.\mathbf{s}} \sum_{m_3} e^{2\pi i m_3 \mathbf{c}.\mathbf{s}}.$$

These three summations over m have a common form:

$$\sum_{m_1=0}^{m_1=M-1} e^{2\pi i m_1 \mathbf{a}.\mathbf{s}} = \frac{\sin \pi M \mathbf{a}.\mathbf{s}}{\sin \pi \mathbf{a}.\mathbf{s}} e^{\pi i (M-1)\mathbf{a}.\mathbf{s}}.$$

For $M = \infty$ or even a moderately large number, this function is virtually zero except when the product $(\mathbf{a}.\mathbf{s})$ is an integer or zero; then, the function has the value of M. For a crystal with one finite dimension and the two other dimensions rather large (e.g. a mica flake), the intensity distribution is given by:

$$I \alpha F^2 \times M_1^2 \times M_2^2 \times \frac{\sin^2 \pi M_3 \mathbf{c}.\mathbf{s}}{\sin^2 \pi \mathbf{c}.\mathbf{s}}.$$

The "interference function" can be simplified further by expressing $\mathbf{s}$ in units of $\mathbf{c}^*$; i.e. $\mathbf{s} = u.\mathbf{c}^*$. Then, the product $\mathbf{c}.\mathbf{s}$ becomes equal to u. By disregarding M_1, M_2 and the subscript of M_3, we are able to reduce the function to the form

$$S^2 = \frac{\sin^2 \pi M u}{\sin^2 \pi u}.$$

The 'interference function' in this form is perfectly general and is independent of any cell parameter (real or reciprocal). The argument (u) of the function represents the fraction of the distance between two consecutive reciprocal lattice points in any direction. This function has been exactly evaluated over a range from single unit-cell thickness to a thickness of 10 unit-cells. The function has been normalized (i.e. S^2/M^2) and plotted in Fig. 2. The numerical values of S^2/M^2 are listed in Table 1.

This function has often been approximated by the expression $\sin x/x$ for which tables are available (Sherman and Brockway, 1959). This approximation has several disadvantages. First, the argument (x) is given in radians and does not directly relate to the reciprocal lattice rows. Second, it only approximates the 'interference function' and therefore deviates appreciably for large values of x.

The 'interference function' ($\sin^2 \pi Mu/\sin^2 \pi u$) is symmetrical at the origin and at $u = \frac{1}{2}$; i.e. $f(u) = f(-u)$ and $f(\frac{1}{2} + u) = f(\frac{1}{2} - u)$. It is, therefore, completely sufficient to list values of the function in the interval $u = 0\text{–}0{\cdot}5$. The "interference function" is also referred to as the shape transform. As seen in Fig. 2, the function is zero at all points with $u = n/M$ and has maxima for $u = (n + \frac{1}{2})/M$, where n is an integer but u remains a fractional number. The elongation of a reflection is usually given by the width of the first maximum $u = 1/M$; that is, the reciprocal of the number of unit-cells in that direction. It is also important to realize that there are additional subsidiary maxima and a strong reflection may therefore have effects farther away on the reciprocal lattice row.

https://doi.org/10.1346/CCMN.1974.0220114 Published online by Cambridge University Press

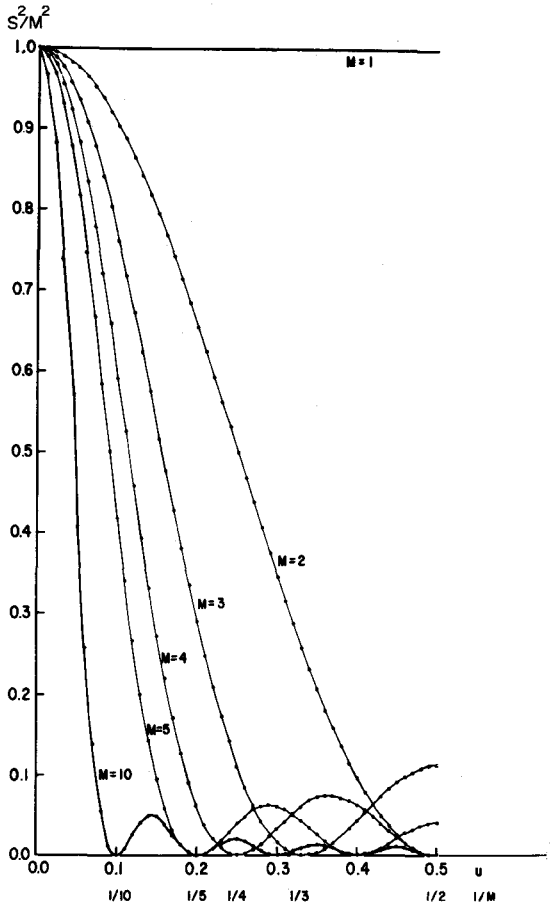


Fig. 2. The normalized interference function of (S^2/M^2) for the M values 1, 2, 3, 4, 5 and 10 (see test).

For a crystal of uniform thickness the 'interference function' affects all the reciprocal lattice points to the same extent as defined by M, number of unit-cells in a given direction. If crystal thickness is not uniform, e.g. wedge-shaped, the interference function will affect each reciprocal lattice point differently corresponding to the values of M in each direction.

Critical thickness

With increasing crystal thickness, the electron diffraction becomes dynamic in nature. The limiting thickness, above which the diffraction is dynamic, is called the critical thickness (t_c). This value is given approximately by the following equation (Murr, 1970):

$$t_c \cong \frac{V_c}{\lambda} \times \frac{1}{F_{hkl}},$$

where V_c is the unit-cell volume (932·6 Å^3 for muscovite). The t_c for muscovite has been calculated for the strongest reflection ($F_{33\bar{1}} = 61{\cdot}5$; see below for the structure factor calculations) and found to be 363 Å for 80 keV.

Ordinarily, for electron diffraction one chooses mica flakes of about 100 Å thickness, a value well below the critical. Kinematical theory of electron diffraction can then be directly applied without worrying about the dynamical effects.

ORIENTATION OF THE CRYSTAL: TILT AND BENDING

The elongation of reciprocal lattice points due to the shape transform gives rise to a range of crystal orientations for which observable intensity may be present. The half angle ($\frac{1}{2}\Delta\alpha$) of the tilt of the crystal is defined by its thickness (t) and the magnitude of the reciprocal lattice vector $|\mathbf{H}|$ by a simple relationship:

$$\tfrac{1}{2}\Delta\alpha \cong \frac{1/t}{|\mathbf{H}|} = \frac{d}{t}.$$

For a mica of 100 Å thickness and for the (11), (02) type reflections with $d = 4{\cdot}50$ Å, $\frac{1}{2}\Delta\alpha \cong 0{\cdot}045$ rad, or 2·5°. Thus, a (11) or (02) type reflection will be observed over a range of tilt of $\pm 2{\cdot}5°$. The range of tilt, similarly calculated, is found to be 1·3° for the (04)-type reflections and 0·65° for the (06)-type reflections.

Bending of mica flakes is rather common and has a similar effect on the SAD pattern. Bending is, however, observed directly by the presence of extinction contours in the electron transmission images.

OBJECTIVE LENS PROPERTIES: DEPTH OF FIELD AND FOCAL LENGTH VARIATIONS

Depth of the field of the objective lens is defined by the expression: $D_{fi} = 2r/\alpha_0$, where r is the radius of the disc of confusion (i.e. the resolution limit), and α_0 is the objective aperture angle. With $r = 10$ Å and $\alpha_0 = 10^{-3}$ rad, the depth of field is found to be about 2 μm for a transmission electron image. In the diffraction mode, the objective aperture is removed and the depth of the field, therefore, is expected to be reduced more than one order in magnitude. Consequently, the focusing conditions become more critical for the diffraction pattern than for the transmission image. If the focusing has been done by examining the transmission image, the diffraction pattern may be off-focus. The depth of the field is still appreciable, however, and allows observation of a finite section of each (hk) row, as indicated in the following paragraphs.

Variations in focal length of the objective lens,

https://doi.org/10.1346/CCMN.1974.0220114 Published online by Cambridge University Press

Table 1. Numerical values for the normalized interference function (S^2/M^2) for the crystal thickness of 2–10 unit-cells

u	$M = 2$	$M = 3$	$M = 4$	$M = 5$	$M = 6$	$M = 7$	$M = 8$	$M = 9$	$M = 10$
0·00	1·0000	1·0000	1·0000	1·0000	1·0000	1·0000	1·0000	1·0000	1·0000
0·01	0·9990	0·9974	0·9951	0·9921	0·9885	0·9843	0·9794	0·9740	0·9678
0·02	0·9961	0·9895	0·9804	0·9688	0·9548	0·9384	0·9198	0·8990	0·8763
0·03	0·9911	0·9765	0·9563	0·9309	0·9005	0·8656	0·8267	0·7843	0·7390
0·04	0·9843	0·9585	0·9234	0·8798	0·8286	0·7713	0·7091	0·6434	0·5758
0·05	0·9755	0·9358	0·8824	0·8173	0·7429	0·6621	0·5775	0·4921	0·4086
0·06	0·9649	0·9086	0·8341	0·7456	0·6477	0·5453	0·4433	0·3461	0·2576
0·07	0·9524	0·8771	0·7798	0·6673	0·5476	0·4284	0·3168	0·2185	0·1375
0·08	0·9382	0·8419	0·7204	0·5850	0·4474	0·3184	0·2068	0·1185	0·0559
0·09	0·9222	0·8032	0·6574	0·5013	0·3513	0·2208	0·1192	0·0501	0·0123
0·10	0·9045	0·7616	0·5920	0·4189	0·2631	0·1399	0·0565	0·0123	0·0000
0·11	0·8853	0·7174	0·5256	0·3401	0·1859	0·0778	0·0185	0·0001	0·0083
0·12	0·8645	0·6713	0·4594	0·2670	0·1217	0·0350	0·0018	0·0056	0·0255
0·13	0·8423	0·6236	0·3947	0·2013	0·0716	0·0101	0·0016	0·0203	0·0415
0·14	0·8187	0·5750	0·3326	0·1444	0·0356	0·0004	0·0117	0·0362	0·0499
0·15	0·7939	0·5259	0·2743	0·0970	0·0129	0·0024	0·0262	0·0476	0·0485
0·16	0·7679	0·4769	0·2205	0·0595	0·0019	0·0119	0·0400	0·0513	0·0390
0·17	0·7409	0·4284	0·1719	0·0318	0·0004	0·0249	0·0494	0·0472	0·0253
0·18	0·7129	0·3809	0·1292	0·0133	0·0060	0·0378	0·0525	0·0372	0·0120
0·19	0·6841	0·3349	0·0927	0·0031	0·0159	0·0479	0·0493	0·0244	0·0030
0·20	0·6545	0·2909	0·0625	0·0000	0·0278	0·0534	0·0409	0·0123	0·0000
0·21	0·6243	0·2491	0·0386	0·0026	0·0393	0·0538	0·0297	0·0038	0·0025
0·22	0·5937	0·2100	0·0208	0·0094	0·0487	0·0494	0·0180	0·0001	0·0085
0·23	0·5627	0·1738	0·0088	0·0189	0·0549	0·0413	0·0083	0·0013	0·0150
0·24	0·5314	0·1408	0·0021	0·0295	0·0572	0·0310	0·0021	0·0061	0·0193
0·25	0·5000	0·1111	0·0000	0·0400	0·0556	0·0204	0·0000	0·0123	0·0200
0·26	0·4686	0·0850	0·0018	0·0493	0·0504	0·0110	0·0018	0·0178	0·0170
0·27	0·4373	0·0624	0·0069	0·0564	0·0427	0·0042	0·0064	0·0209	0·0116
0·28	0·4063	0·0434	0·0143	0·0609	0·0334	0·0005	0·0123	0·0207	0·0058
0·29	0·3757	0·0281	0·0232	0·0625	0·0236	0·0003	0·0178	0·0175	0·0015
0·30	0·3455	0·0162	0·0330	0·0611	0·0147	0·0030	0·0216	0·0123	0·0000
0·31	0·3159	0·0077	0·0428	0·0570	0·0074	0·0077	0·0228	0·0068	0·0014
0·32	0·2871	0·0024	0·0521	0·0508	0·0024	0·0134	0·0211	0·0023	0·0048
0·33	0·2591	0·0001	0·0601	0·0429	0·0001	0·0188	0·0173	0·0001	0·0088
0·34	0·2321	0·0006	0·0666	0·0341	0·0006	0·0230	0·0121	0·0006	0·0118
0·35	0·2061	0·0034	0·0712	0·0252	0·0033	0·0251	0·0068	0·0032	0·0126
0·36	0·1813	0·0084	0·0737	0·0169	0·0079	0·0248	0·0026	0·0071	0·0110
0·37	0·1577	0·0151	0·0739	0·0098	0·0134	0·0223	0·0003	0·0109	0·0078
0·38	0·1355	0·0233	0·0720	0·0044	0·0191	0·0181	0·0003	0·0134	0·0040
0·39	0·1147	0·0325	0·0681	0·0011	0·0241	0·0130	0·0024	0·0139	0·0011
0·40	0·0955	0·0424	0·0625	0·0000	0·0278	0·0078	0·0060	0·0123	0·0000
0·41	0·0778	0·0527	0·0555	0·0011	0·0296	0·0035	0·0101	0·0092	0·0010
0·42	0·0618	0·0629	0·0475	0·0041	0·0295	0·0008	0·0136	0·0053	0·0037
0·43	0·0476	0·0728	0·0390	0·0087	0·0274	0·0000	0·0158	0·0020	0·0069
0·44	0·0351	0·0821	0·0304	0·0143	0·0236	0·0013	0·0161	0·0002	0·0094
0·45	0·0245	0·0904	0·0221	0·0205	0·0186	0·0043	0·0145	0·0003	0·0103
0·46	0·0157	0·0976	0·0147	0·0266	0·0132	0·0084	0·0113	0·0023	0·0092
0·47	0·0089	0·1034	0·0085	0·0320	0·0080	0·0129	0·0074	0·0054	0·0066
0·48	0·0039	0·1076	0·0039	0·0363	0·0038	0·0168	0·0036	0·0088	0·0035
0·49	0·0010	0·1102	0·0010	0·0391	0·0010	0·0195	0·0010	0·0114	0·0010
0·50	0·0000	0·1111	0·0000	0·0400	0·0000	0·0204	0·0000	0·0123	0·0000

The u values are given in fractions of the distance between two consecutive reciprocal lattice points along any direction. For $M = 1$ the function is unity for all values of u.

achieved by changing the lens current, significantly modify the SAD pattern. In Figs. 3(a–d), the effects of such focal length variation on the spot intensities of SAD can be easily followed. As an example, let us examine the (11), ($\bar{1}$1), ($\bar{1}\bar{1}$) and (1$\bar{1}$) reflections. Figure 3(a) shows that the (11) reflection is significantly stronger than the others and that there is no center of symmetry in this pattern. As the focal length is slightly changed, the intensities of the (11) reflections are modified because a different section of the reciprocal lattice is

https://doi.org/10.1346/CCMN.1974.0220114 Published online by Cambridge University Press

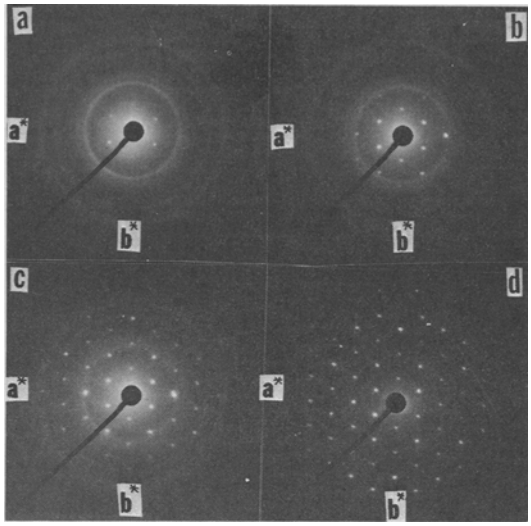


Fig. 3(a–d). The changes is SAD patterns of $2M_1$ muscovite at the variations of objective lens current: The focal length is increased from (*a* to *d*). The uniform rings are from the gold coating.

now observed (Fig. 3b). The (11) reflections have now approximately equal intensities and the six reflections (02 and 11 type) display a symmetry close to 2/*m*. This symmetry, however, is not valid for the other spots in the figure, which are now appearing up to $h = 2$ and $k = 4$. From these, (20) and (13) reflections are rather well observed. The intensity of the $(\bar{2}0)$ is much stronger than that of the (20) spot. Similarly the $(\bar{1}3)$ reflection is markedly stronger than the $(1\bar{3})$. With further decrease in objective lens current, we obtain Fig. 3(c). At this focal length the intensities of the (20) and (13) reflections have significantly changed. The (20) reflection has become much stronger and its intensity is rather close to that of $(\bar{2}0)$. Similarly, the $(\bar{1}3)$ and $(1\bar{3})$ reflections now have almost equal intensities. It is interesting to notice on Fig. 3(c) that the (06) and (33) reflections, which appear at this focal length, have rather unusual intensity relationships. The $(0\bar{6})$ is much stronger than the (06) reflection, indicating that the *a*–*b* plane of the mica is slightly tilted. On the micrograph (Fig. 3d) obtained after further decreasing objective lens current, the (06) and $(0\bar{6})$ reflections become of almost equal intensity. This result indicates that the depth of the field of the objective lens must still be appreciable in the diffraction mode in order to compensate for the slight tilt.

In conclusion, we may state that the focusing conditions are rather critical and *the symmetry determination of the SAD patterns requires a focal series.* The variations in focal length give us on the other hand the possibility of scanning to a limited extent the intensity distribution along the reciprocal lattice rods.

COMPARISON BETWEEN EXPERIMENTAL AND THEORETICAL INTENSITY VARIATIONS ON SAD PATTERNS OF $2M_1$ MUSCOVITE

In the previous sections the factors which could cause intensity variation have been described. In this section the intensities for the (*hk*) spots of a $2M_1$ muscovite flake about 100 Å thick ($M = 5$) will be calculated and compared to the observed values. Because of the very small c^* parameter of the crystal we may consider for each (*hk*) spot the three reciprocal lattice points close to the Ewald sphere (Fig. 1a). We call this part of the (*hk*) row the 'excitation region' for the (*hk*) reflection on SAD patterns. These three reflections have been listed in Table 2 with their characteristic values: Δp, $\Delta s'$, ζ and $|F_{hkl}|^2$. The first three variables are given in fractions of the reciprocal cell parameter c^*.

The reciprocal lattice points are plotted in Fig. 4 with respect to a reference plane $\zeta = 0$ which indicates exactly where the Ewald sphere intersects each (*hk*) row. Thus, the excitation errors (ζ) of each reciprocal lattice point are given by the distance to that plane. If the objective lens is exactly in-focus during the diffraction, the expected SAD pattern should represent the section of the reciprocal lattice at $\zeta = 0$. The effect of variations in focal length of the objective lens can be visualized by observing sections of the reciprocal lattice at different ζ values.

In order to find out which section of the reciprocal lattice is in-focus, we have to consider the continuous intensity distribution along each (*hk*) row. For this purpose, structure factors have been calculated using fractional *l* indices, where *l* varies with increments of $\Delta l = 0{\cdot}1$ from the *l* index of the first reflection to the *l* index of the last one in a row. Similarly the interference function has been evaluated for each point corresponding to the fractional or integer *l* values along the same row. The intensities have been calculated using the expression $I = F^2 \times (S/M)^2$ and the obtained values of *F* and (*S*/*M*). The results are plotted in Fig. 4. In case of symmetrical rows, e.g. (11) and $(\bar{1}1)$ rows for $2M_1$ muscovite, the intensity distribution has been computed for one of the rows and the other is derived from it by the symmetry. Atomic scattering factors for electrons (Ibers and Vainstein, 1962) and atomic cell parameters reported by Güven (1971) have been used for the structure factor calculations. The scattering factors have been, however, corrected for the accelerating voltage (80 keV) by multiplying by the relativity factor $m/m_0 = (1 - v^2c^2)^{-1/2} = 1{\cdot}1566$.

We can easily follow the behavior of SAD patterns with different focusing conditions by comparing Fig. 4 with Figs. 3(a–d). If we, for instance, compare the intensities for (20) and $(\bar{2}0)$ reflections on both figures, it

https://doi.org/10.1346/CCMN.1974.0220114 Published online by Cambridge University Press

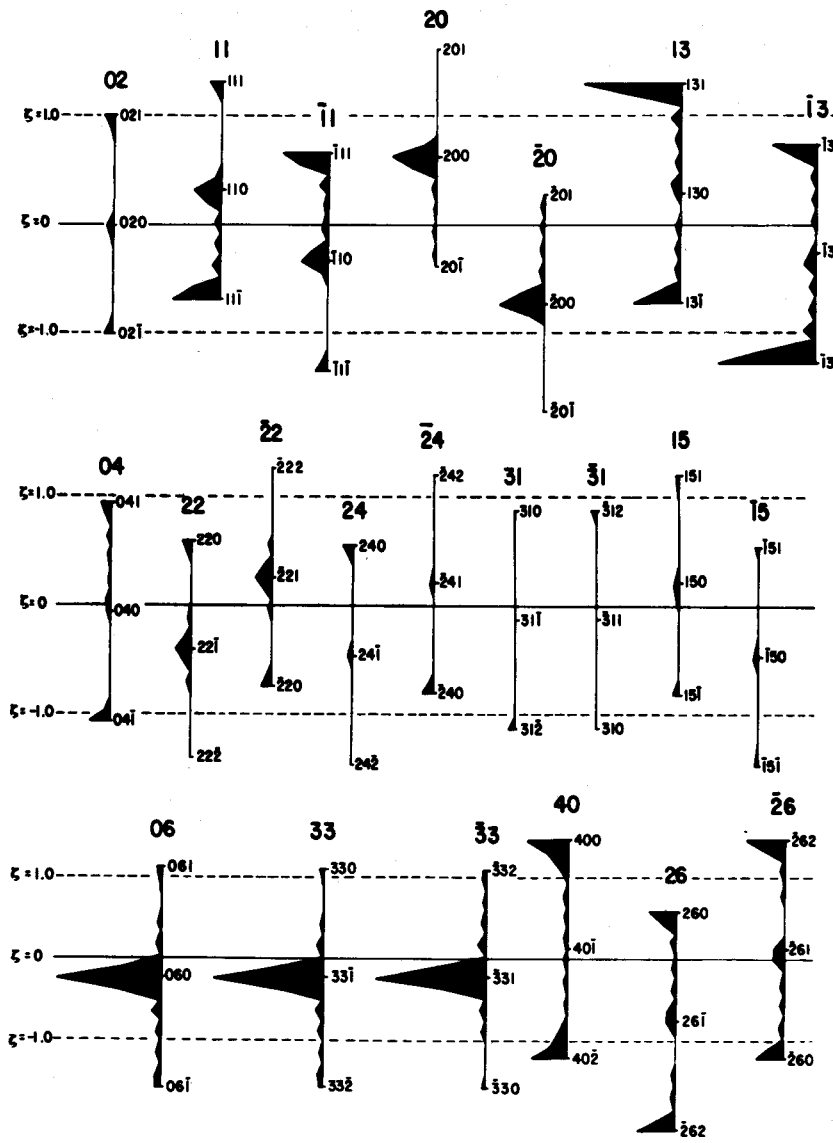


Fig. 4. SAD intensity variations along the (*hk*) rows in the 'excitation region' for $2M_1$ muscovite of 100 Å thickness (see text).

will become obvious that the SAD image in Fig. 3(b) is focused somewhere between $\zeta = 0$ and $\zeta = -1{\cdot}0$. The SAD image in Fig. 3(d), obtained after the objective focal length was decreased, is now focused somewhere in the region $\zeta = 0{\cdot}0$ and $\zeta = 1{\cdot}0$. The fact that the intensities of these spots are rather close to each other in Fig. 3(c) is important. This indicates that the (20) and ($\bar{2}0$) spots are receiving quite a portion of diffracted electrons from the vicinity of the (200) and ($\bar{2}00$) reciprocal lattice points (see Fig. 4). This circumstance may be possible if the depth of field in the diffraction mode is still appreciable, because the vertical distance between these reciprocal lattice points is equal to the sum: $\zeta_{200} + \zeta_{\bar{2}00} = (4/3) \times c^* = 0{\cdot}07\ \text{Å}^{-1}$. Similarly, the intensity variations of the (11) and ($\bar{1}1$) or other reflections can be explained. Thus, the scattered electrons do not originate just from a point along an (*hk*) row but from a 'finite' vertical portion determined by the depth of field and by the actual focal plane of the objective lens. The observed intensity on the SAD pattern is the integrated energy from that vertical portion. Further experimental and theoretical work is needed to find the exact values of these properties of the objective lens for each diffraction pattern. At this point, it

https://doi.org/10.1346/CCMN.1974.0220114 Published online by Cambridge University Press

Table 2. Characteristic data for the three reciprocal lattice points in the 'excitation region' for each *hk*-spot on the SAD pattern (see text)

hk Indices	Three *r.l.* points in the excitation region	Δp	$\Delta s'$	$\zeta = \Delta p - \Delta s'$	$\lvert F_{hkl}\rvert^2$ (normalized to $I_{33\bar{1}} = 100$)
	0 2 1	1·0	0·02	0·98	7
02	0 2 0	0·0	0·02	−0·02	4
	0 2 $\bar{1}$	−1·0	0·02	−1·02	7
	1 1 1	4/3	0·02	1·31	10
11	1 1 0	1/3	0·02	0·31	18
	1 1 $\bar{1}$	−2/3	0·02	−0·69	43
	$\bar{1}$ 1 1	2/3	0·02	0·65	43
$\bar{1}$1	$\bar{1}$ 1 0	−1/3	0·02	−0·35	18
	$\bar{1}$ 1 $\bar{1}$	−4/3	0·02	−1·35	10
	2 0 1	5/3	0·06	1·61	0
20	2 0 0	2/3	0·06	0·61	38
	2 0 $\bar{1}$	−1/3	0·06	−0·39	0
	1 3 1	4/3	0·06	1·27	88
13	1 3 0	1/3	0·06	0·27	5
	1 3 $\bar{1}$	−2/3	0·06	−0·73	39
	$\bar{1}$ 3 1	2/3	0·06	0·61	39
$\bar{1}$3	$\bar{1}$ 3 0	−1/3	0·06	−0·39	5
	$\bar{1}$ 3 $\bar{1}$	−4/3	0·06	−1·39	88
	0 4 1	1·0	0·08	0·92	6
04	0 4 0	0·0	0·08	−0·08	2
	0 4 $\bar{1}$	−1·0	0·08	−1·08	6
	2 2 0	2/3	0·08	0·59	7
22	2 2 $\bar{1}$	−1/3	0·08	−0·41	13
	2 2 $\bar{2}$	−4/3	0·08	−1·41	0
	$\bar{2}$ 2 2	4/3	0·08	1·25	0
$\bar{2}$2	$\bar{2}$ 2 1	1/3	0·08	0·25	13
	$\bar{2}$ 2 0	−2/3	0·08	−0·75	7
	2 4 0	2/3	0·14	0·53	7
24	2 4 $\bar{1}$	−1/3	0·14	−0·47	1
	2 4 $\bar{2}$	−4/3	0·14	−1·47	0
	$\bar{2}$ 4 2	4/3	0·14	1·19	0
$\bar{2}$4	$\bar{2}$ 4 1	1/3	0·14	0·19	1
	$\bar{2}$ 4 0	−2/3	0·14	−0·81	7
	3 1 0	1·0	0·14	0·86	0
31	3 1 $\bar{1}$	0·0	0·14	−0·14	0
	3 1 $\bar{2}$	−1·0	0·14	−1·14	3
	$\bar{3}$ 1 2	1·0	0·14	0·86	3
$\bar{3}$1	$\bar{3}$ 1 1	0·0	0·14	−0·14	0
	$\bar{3}$ 1 0	−1·0	0·14	−1·14	0
	1 5 1	4/3	0·14	1·19	2
15	1 5 0	1/3	0·14	0·19	2
	1 5 $\bar{1}$	−2/3	0·14	−0·81	1
	$\bar{1}$ 5 1	2/3	0·14	0·53	1
$\bar{1}$5	$\bar{1}$ 5 0	−1/3	0·14	−0·47	2
	$\bar{1}$ 5 $\bar{1}$	−4/3	0·14	−1·47	2
	0 6 1	1·0	0·18	0·82	4
06	0 6 0	0·0	0·18	−0·18	95
	0 6 $\bar{1}$	−1·0	0·18	−1·18	4
	3 3 $\bar{2}$	−1·0	0·18	−1·18	1
33	3 3 $\bar{1}$	0·0	0·18	−0·18	100
	3 3 0	1·0	0·18	0·82	1

https://doi.org/10.1346/CCMN.1974.0220114 Published online by Cambridge University Press

Table 2. cont.

hk Indices	Three *r.l.* points in the excitation region	Δp	$\Delta s'$	$\zeta = \Delta p - \Delta s'$	$\lvert F_{hkl}\rvert^2$ (normalized to $I_{33\bar{1}} = 100$)
	$\bar{3}\,3\,0$	−1·0	0·18	−1·18	1
$\bar{3}3$	$\bar{3}\,3\,1$	0·0	0·18	−0·18	100
	$\bar{3}\,3\,2$	1·0	0·18	0·82	1
	$4\,0\,0$	4/3	0·24	1·09	35
40	$4\,0\,\bar{1}$	1/3	0·24	0·09	0
	$4\,0\,\bar{2}$	−2/3	0·24	−0·91	30
	$2\,6\,0$	2/3	0·24	0·43	24
26	$2\,6\,\bar{1}$	−1/3	0·24	−0·57	7
	$2\,6\,\bar{2}$	−4/3	0·24	−1·57	33
	$\bar{2}\,6\,2$	4/3	0·24	1·09	33
$\bar{2}6$	$\bar{2}\,6\,1$	1/3	0·24	0·09	7
	$\bar{2}\,6\,0$	−2/3	0·24	−0·91	24

is relevant to point out for intensity calculations the possible error in the assumption that the SAD represents just a planar section of the reciprocal lattice. This assumption may be a grave mistake especially for crystals like micas which possess a very small reciprocal lattice parameter in the direction of the electron beam. In fact, I have not been able to find agreement between the observed and calculated SAD intensities for $2M_1$ muscovite on such an assumption.

DISCREPANCIES BETWEEN SAD SYMMETRY AND CRYSTAL SYMMETRY

As was derived by Vainstein (1964), only six different plane point groups may be observed on the SAD patterns. These are: 2; 2*mm*; 4; 4*mm*; 6; and 6*mm*. Physical, geometrical and instrumental factors may sometimes give rise to deviations in SAD patterns from these symmetries. We will consider only the deviations caused by the factors discussed in this paper.

In general, the symmetry related reciprocal lattice points are expected to have equal intensities on the SAD pattern if their excitation errors ζ (i.e. their distances from the Ewald sphere) are equal. This expectation may not always obtain for crystals with monoclinic and triclinic symmetry, even under ideal focusing conditions without any tilt or bending. In such cases, we need in fact to have a certain amount of tilt to observe the symmetry. In monoclinic crystals, only the symmetrical reciprocal lattice points with $\Delta p = 0$, (i.e. $h/3 + l = 0$) like (020) and ($0\bar{2}0$), have equal distances to the Ewald sphere. The well-known relationship (Friedel's symmetry) in diffraction, $I_{hk} = I_{\bar{h}\bar{k}}$, may not be observed because of different ζ values of the centrosymmetrical reciprocal lattice points. Under non-ideal conditions (i.e. the objective lens off-focus and the presence of tilt or bending, non-uniform thickness) SAD symmetry will deviate from the crystal symmetry as discussed above. The plane point group 2*mm* of $2M_1$ muscovite may then be reduced to all the possible subgroup symmetries such as *m*, 2, $\bar{1}$ and 1. The deviation from the actual symmetry would be more pronounced for spots with larger indices, as the difference in excitation errors (ζ) for the symmetrical reflections becomes larger.

Another interesting feature of $2M_1$ muscovite is the fact that the (02) and ($0\bar{2}$) reflections are significantly weaker than the (11) reflections. Even a change in focusing conditions and considerable tilt (up to 2·5° for 100 Å thickness) do not cause any appreciable changes in the intensities of (02) reflections. This is not the case for other micas or for other layer silicates. These reflections form SAD diagnostic criteria for $2M_1$ type dioctahedral layer silicates.

Acknowledgements—I thank Mr. Rodney W. Pease, Department of Geosciences, Texas Technical University, for helping me in proper usage of English in the manuscript.

REFERENCES

Cowley, J. M. (1967) Crystal structure determination by electron diffraction. In *Progress in Materials Science*, (Edited by Chalmers, B. and Hume-Rothery, W.), **13,** 269–321, Pergamon Press, Oxford.

Güven, N. (1971) The crystal structures of $2M_1$ phengite and $2M_1$ muscovite: *Z. Kristallogr.* **134,** 196–212.

Ibers, J. A. and Vainstein, B. K. (1968) In *International Crystallographic Tables*, (Edited by Lonsdale, K.), Volume III, Tables 3.3.3.A(1), pp. 218–219. Kynoch Press, Birmingham.

Murr, L. E. (1970) *Electron Optical Applications in Materials Science*, p. 259. McGraw-Hill, New York.

Pinsker, Z. G. (1953) *Electron Diffraction*. Butterworth, London.

https://doi.org/10.1346/CCMN.1974.0220114 Published online by Cambridge University Press

Rothbauer, R. (1971) Untersuchung eines $2M_1$-Muscovite mit Neutronenstrahlen: *N. Jb. Miner. Mh.* **4,** 143–154.

Sherman, J., assisted by Brockway, L. (1959) In *International Crystallographic Tables,* (Edited by Kasper, J. S. and Lonsdale, K.), Volume II, Table 8.2A p. 366. Kynoch Press, Birmingham.

Vainstein, B. K. (1964) *Structure Analysis by Electron Diffraction.* Pergamon Press, Oxford.

Résumé—Les facteurs principaux qui affectent les diagrammes de micro-diffraction électronique (SAD) des micas sont: les propriétés de réseau du cristal, l'épaisseur de l'échantillon, l'orientation du cristal, les propriétes de la sphère d'Ewald vis-à-vis de la diffraction électronique, la profondeur de champ de la lentille objectif et les variations dans les conditions de focalisation de cette lentille. Sous la dépendance de ces facteurs, les diagrammes SAD de muscovite 2 M_1 peuvent montrer différentes symétries. L'épaisseur 'finie' de l'échantillon affecte l'intensité en termes de la 'fonction d'interférence'. Cette fonction a été exactement évaluée et la distribution d'intensité a été calculée le long des rangées (*hk*). Les variations d'intensité observées pour les taches (*hk*) indiquent que les conditions de focalisation de la lentille objectif sont assez critiques pour la symétrie des diagrammes SAD.

Kurzreferat—Die wichtigsten Faktoren, die die Feinbereichselektronenbeugungs-(SAD)-Diagramme von Glimmer beeinflussen, sind: Gittereigenschaften des Kristalles, Probendicke, Orientierung des Kristalles, Eigenschaften der Ewald-Kugel für die Elektronenbeugung, Tiefenschärfe der Objektivlinse und Veränderungen der Fokussierungsbedingungen dieser Linse.

In Abhängigkeit von diesen Faktoren können die SAD-Diagramme von 2 M_1-Muskovit verschiedene Symmetrien aufweisen. 'Endliche' Dicke der Proben beeinflußt die Intensität nach den Bedingungen der 'Interferenzfunktion'. Diese Funktion wurde genau bestimmt und die Intensitätsverteilung entlang den (*h k*)-Reihen berechnet. Die beobachteten Intensitätsveränderungen der (*h k*)-Flecken zeigten, daß die Fokussierungsbedingungen der Objektivlinse für die Symmetrie der SAD-Diagramme sehr kritisch sind.

Резюме — Главные факторы влияющие на электронограммы выбранных образцов слюды являются: свойства решетки кристалла, толщина образца, ориентировка кристалла, способность шарового фотометра Эвальда к дифракции электронов, глубина поля линзы объектива и колебательные состояние фокусирования этой линзы. В зависимости от этих факторов электронограммы $2M_1$ московита могут показывать различные симметрии. «Финитная» толщина образца влияет на интенсивность в смысле «явления интерференции». Последнее явление точно оценивалось и высчитывалось распределение интенсивности по рядам (hk). Наблюдаемая вариация интенсивности точек (hk) указывает, что состояния фокусирований линзы объектива являются довольно критическими для симметрии электронограмм.

https://doi.org/10.1346/CCMN.1974.0220114 Published online by Cambridge University Press